BUNDESREPUBLIK
DEUTSCHLAND

Bundesanstalt für
Geowissenschaften und
Rohstoffe (BGR)

Hannover

REPUBLIQUE
DE DJIBOUTI

Office Djiboutien de
Développement de
l'Énergie Géothermique
(ODDEG)

Djibouti

Regional Project

Geothermal Energy East Africa

Lineament Mapping in North Ghoubbet (Tadjoura, Djibouti)

Alina Ermertz

Remote Sensing Working Group BGR

Hannover, October 2020

Lineament Mapping in North Ghoubbet (Tadjoura, Djibouti)

Author	Alina Ermertz (BGR)

Project Number	2016.2066.5
BGR Number	05-2392
Project Partner (ODDEG)	Office Djiboutien de Développement de l’Énergie Géothermique
Pages	31
Place and date of issuance	Hannover, October 2020

Abbreviations
List of figures
Summary

Table of Contents

Table of waypoints with map
Quantum GIS Project DVD

Abbreviations

BGR	Bundesanstalt für Geowissenschaften und Rohstoffe (Federal Institute for Geosciences and Natural Resources)
BGRM	Bureau de Recherches Géologiques et Minières
DEM	Digital Elevation Model
GIS	Geographic Information System
GPS	Global Positioning System
InSAR	Interferometric Synthetic Aperture Radar
IW	Interferometric Wide Swath
m asl	Meters above sea level
MSI	Multispectral Instrument
ODDEG	Office Djiboutien de Développement de l'Énergie Géothermique
RGB	Red Green Blue (colour band combination)
SRTM	Shuttle Radar Topography Mission
WP	Waypoint (measured by GPS)

List of figures

Summary

Within the technical cooperation project “Geothermal Energy in East Africa”, recent work focusses on the cooperation with the project partner *Office Djiboutien de Développement de l’Énergie Géothermique* (ODDEG) in Djibouti. One part of the collaboration includes the use of remote sensing data for geothermal exploration.

Current exploration work is conducted in the study area *North Ghoubbet* in central Djibouti. Multispectral satellite imagery and digital elevation models are used for a lineament analysis of the area, as this knowledge is of major importance for exploring a geothermal site. Faults are expressed through lineaments on the earth’s surface. A high density of lineaments therefore indicates areas that favor the circulation of hydrothermal fluids and that are appropriate for further exploration.

In this context, freely available multispectral Sentinel-2 and SRTM digital elevation data are used for the structural analysis. Lineament mapping has been conducted prior to field investigations, so that findings in the field could directly be correlated with the structural setting. The fieldwork was carried out with partners from the project partner ODDEG in February 2020. Detailed lineament mapping and interpretation is executed with knowledge from the field, including an assessment of the activity of specific tectonic structures based on the occurrence of geothermal manifestations.

The active NW-SE oriented Asal-Ghoubbet rift controls the structural setting of *North Ghoubbet*, being located in the southwest of the study area. Faults primarily occur in the direction of this rift system, striking NW-SE. The location of the N(NW)-S(SE) striking Makarassou Fault Zone to the northwest of *North Ghoubbet* additionally leads to the development of N(NW)-S(SE) structures. Especially the central and eastern parts of the study area are characterized by a dense lineament network with a large amount of major structures. Recommended areas for further exploration are located in these parts of *North Ghoubbet.*

1 Scope of the Work

In context of the regional project “Geothermal Energy in East Africa”, several studies have been conducted in Djibouti. The BGR supports the exploration of geothermal sites in different fields of expertise. There is no productive geothermal plant so far, but the potential is considered highly promising at several sites. The project partner *Office Djiboutien de Développement de l’Energie Géothermique* (ODDEG) defined 22 sites in different regions of the country for further exploration in the near future. The government aims to get independent in terms of electricity production, as most of the electricity is presently imported from Ethiopia. The long-term aim is to cover the electricity production completely by renewable resources and in this context to extend the geothermal sector.

Remote sensing methods are applied to assist the exploration in the study area *North Ghoubbet* in the region of Tadjoura. Structural mapping is performed based on multispectral products and digital elevation models. Tectonic studies are of major importance for estimating the geothermal potential, as faults act as pathways for hydrothermal fluids and a high density of faults increases the permeability and in turn the potential of a geothermal system.

The aim of this work is to define areas where tectonic structures indicate a high permeability for fluids and where faults show a high activity. A first verification of the remote sensing work was conducted together with partners from ODDEG in February 2020 (10/02/2020 to 12/02/2020).

2 Geothermal Exploration in the Republic of Djibouti

Geothermal exploration studies in Djibouti were conducted since the 1970's in different periods and at different sites (Aden et al. 2018, Zan et al. 1990). The French geological survey *Bureau de Recherches Géologiques et Minières* (BRGM) carried out first studies in the 1970's in the Asal area by drilling two deep wells. In the same area, a second exploration period was realized in the late 80's with an Italian company drilling another four deep wells. The maximum reached depth for the deep wells is 2105 m. Another shallow well of approximately 1300 m was drilled 2016 by the Turkish company PARS (Aden et al. 2018). Three of these six deep wells were productive, but the high salinity of geothermal fluids caused problems due to mineral scaling and corrosion of the equipment (Houssein & Axelsson 2010).

Although the Asal area is characterized by a suitable heat source with temperatures ranging between 260°C-360°C, the salty fluid composition is a major problem during the production (Aden et al. 2018, Houssein & Axelsson 2010). The North Ghoubbet area is thought to be a promising site, as a high geothermal potential exists and the reservoir is fed by meteoric water of the Goda Mountains rather than saline waters from the sea.

In addition to the exploration of the North Ghoubbet area, three more areas are currently explored. They are located in *Arta*, east of Lac du Ghoubbet, *Hanlé* in western Djibouti and *Lac Abhé* in southwestern Djibouti close to the Ethiopian border.

3 Working Area

Djibouti is located in the northeastern part of the African continent, which is also referred to as the Horn of Africa. The working area *North Ghoubbet* covers 161 km² in the central part of Djibouti in the region of Tadjoura (Figure 3.1). Lake Ghoubbet borders the study area to the south.

Elevations range from 0 m above sea level at the coast to approximately 575 m above sea level in the central part of the *North Ghoubbet*. Mountains belonging to the Goda Mountain Range lie a few kilometers north of the study area, feeding this area with meteoric waters. Extensive wadi systems also occur in the central part and are easily visible on the satellite imagery (Figure 3.1b).

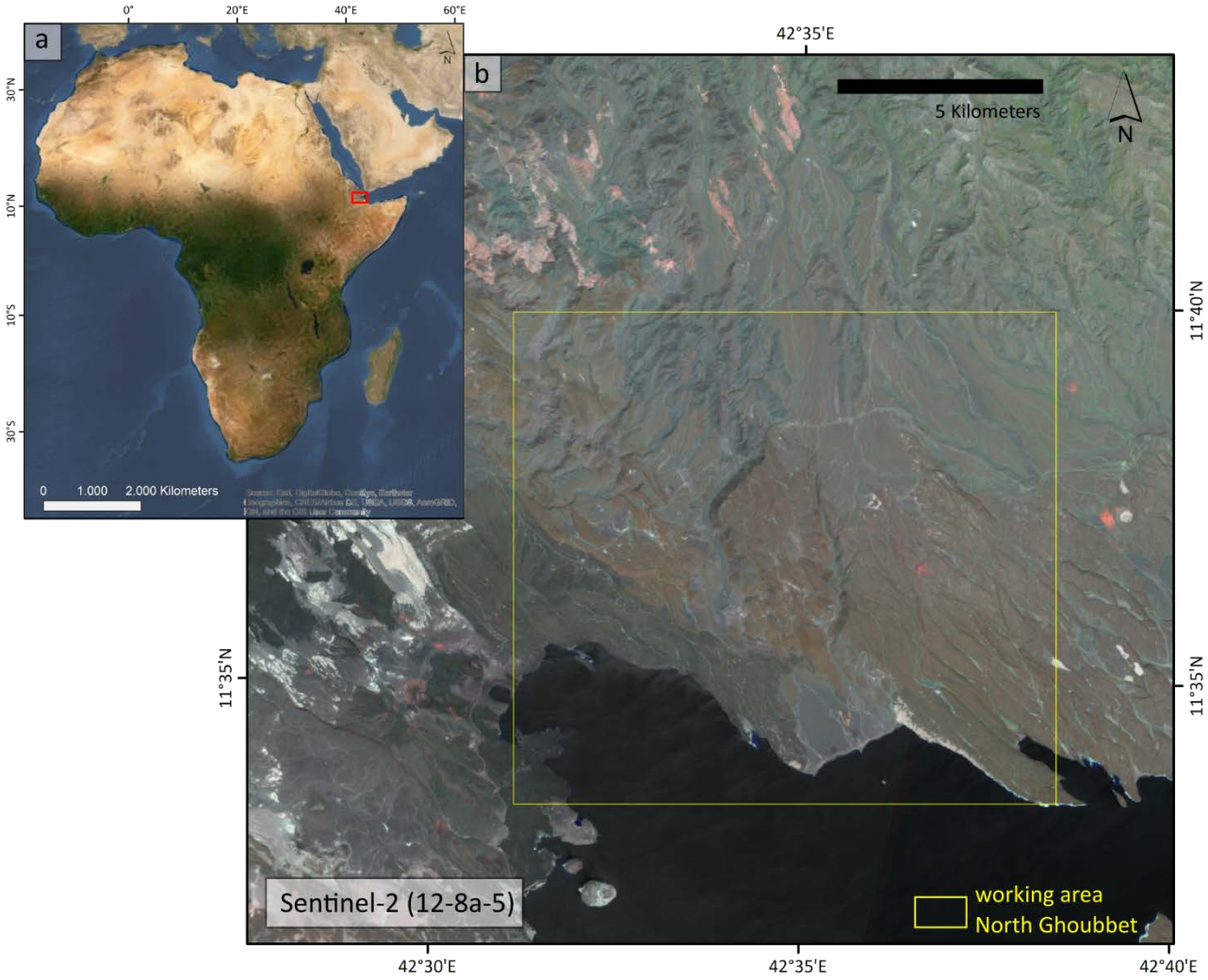

Figure 3.1: (a) Red rectangle represents the location of Djibouti on the African continent. (b) Extent of the working area North Ghoubbet in central Djibouti, displayed on a Sentinel 2A scene from 23.10.2019, bands 12-8a-5 (RGB) (Contains modified Copernicus Sentinel data 2019).

4 Geology & Plate Tectonic Setting

4.1 Geology of the Afar Triangle

Djibouti is part of the Afar Triangle, where the Nubian and Somalian Plate and the Arabian Plate meet and form a huge depression, the Afar Triple Junction (Chorowicz 2005; Figure 4.1). The divergent plate boundary between the Nubian and Somalian Plate forms the East African Rift System that extends from the Afar Triple Junction southward and continues to Mozambique in southeast Africa. The Nubian and Arabian Plates drift apart along the Red Sea and the Arabian and Somalian plate boundary is represented by the Gulf of Aden, both connected by the Bab-el-Mandeb strait off the Djiboutian coast (Figure 4.1).

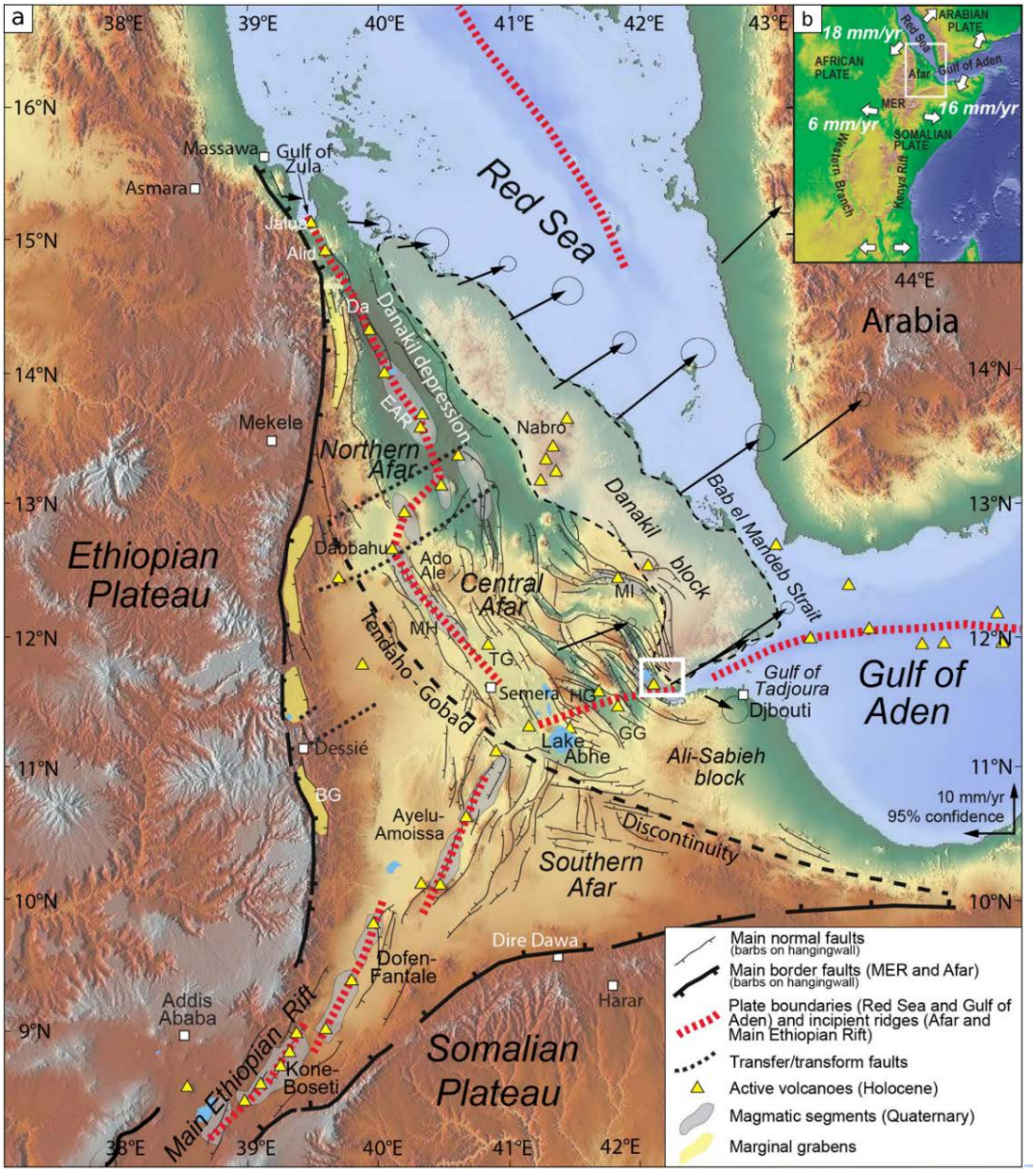

Figure 4.1: (a) Topography of the Afar Triple Junction based on SRTM data (modified after Sani et al. 2017). The white rectangle shows the location of the study area which lies in the central part of the Afar Triangle. (b) Location of the Afar Triple Junction with averaged velocity and direction of rift opening.

Continental rifting in the three rift branches started in Oligocene times (Collet et al. 2000, Sani et al. 2017). The Nubian-Somalian divergence is roughly oriented WNW-ESE with spreading rates of approximately 6 mm per year, while the opening of the Red Sea and Gulf of Aden is oriented NE or, respectively, NNE with spreading rates of approximately 17 mm per year (Eagles et al. 2002, Sani et al. 2017, Vigny et al. 2007; Figure 4.1b). Hence, major tectonic structures are oriented NNE-SSW like the East African Rift System and NW-SE following the Red Sea direction, turning into a more E-W trend corresponding to the Gulf of Aden.

The first stages of extension lead to thinning of the continental crust and consequently, to the development of the Danakil depression in the northwestern part of the Afar Triangle, which separates the Danakil block in the East from the Nubian Plate in the West (Beyene & Abdelsalam 2005, Sani et al. 2017; Figure 4.1a). Counterclockwise rotation of the Danakil block continued through Miocene and Pliocene times until today and influences the tectonic regime of the area (Collet et al. 2000, Eagles et al. 2002, McClusky et al. 2010, Polun et al. 2018). To the south, the Danakil block is separated from the Somalian Plate by the Gulf of Aden Rift and the Gulf of Tadjoura including the Ghoubbet-Asal Rift as its westward elongation (Beyene & Abdelsalam 2005, Eagles et al. 2002).

Opening of the Asal-Rift began in early Quaternary times, around 853 ky ago (Pinzuti et al. 2010). Present opening rates account for approximately 16 mm to 17 mm per year in the northeastern direction (40°) (Pinzuti et al. 2010, Vigny et al. 2007). The opening is not constant but rather affected by several rifting events (Vigny et al. 2007). Intense studies of displacements and movement directions along the Asal Rift indicate that the opening of the Asal-Ghoubbet rift accommodates for most of the divergence between the Arabian and Somalian Plates (Doubre & Peltzer 2007; Vigny et al. 2007).

Geological Units

The geological units of the Afar Triangle mainly consist of Cenozoic sedimentary and volcanic rocks (Schlüter 2008, Vellutini 1990; Figure 4.2). The Neoproterozoic basement is overlain by a cover of Mesozoic sandstones and limestones that occur in the marginal part of the Afar Depression (Beyene & Abdelsalam 2005). In late Mesozoic times, the first volcanism since Neoproterozoic times occurred, also in the marginal parts of the Afar Triangle (Beyene & Abdelsalam 2005). Volcanic deposits of different phases that erupted throughout the Eocene and Miocene occur in several parts of the Afar Depression (Beyene & Abdelsalam 2005). These include rhyolites of the Mabla Series and basalts of the Dalha Series that occur in the area around the Gulf of Tadjoura (Beyene & Abdelsalam 2005, Vellutini 1990).

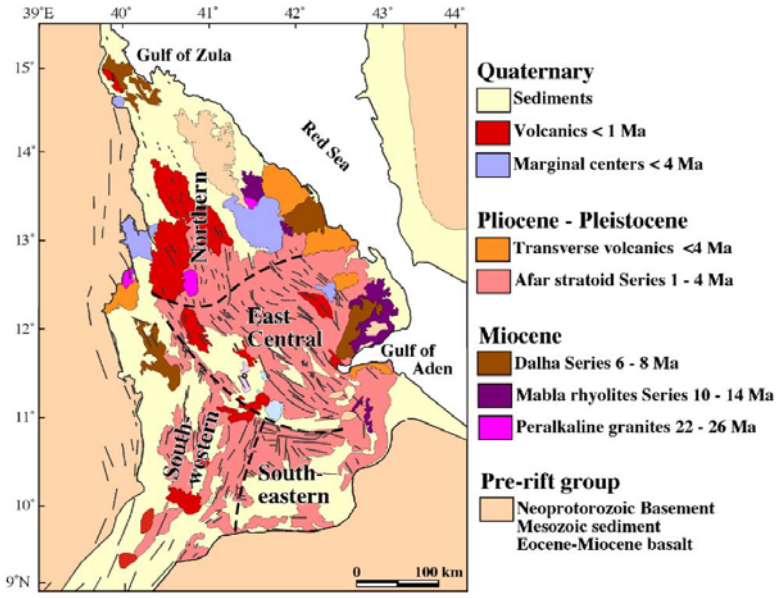

Figure 4.2: Gelogical map of the Afar Depression (Beyene & Abdelsalam 2005). The depression can be divided into Northern, East Central, Southwestern and Southeastern regions, based on their structural trends, with Djibouti lying in the East Central region.

Most parts of the Afar Depression are covered by volcanic rocks of Pliocene-Pleistocene age, being part of the basaltic Stratoid Series that covers large parts of the Djiboutian territory, as to be seen on the geological map in Figure 4.3 (Beyene & Abdelsalam 2005, Vellutini 1990). Synchronous to the eruption of the Stratoid Series flood basalts around 4-1 Ma ago, basalts were erupted along with the opening of the Gulf of Tadjoura, in this context referred to as Basalts of the Gulf (Vellutini 1990; Figure 4.3). The youngest deposits of the country are represented by the Rift Basalts that erupted in the two rift systems Manda Inakir and Asal-Ghoubbet during the Quaternary (de Chabalier & Avouac 1994; Figure 4.3).

In the Asal-Ghoubbet Rift system, these young volcanics were erupted by the Fieale volcano in three subsequent phases throughout the Quaternary and form the modern structure of the rift (de Chabalier & Avouac 1994, Pinzuti et al. 2010). Since appr. 40-30 ky ago, the magmatic activity is located along small volcanic structures and eruptive fissures in the inner floor of the rift (Pinzuti et al. 2010).

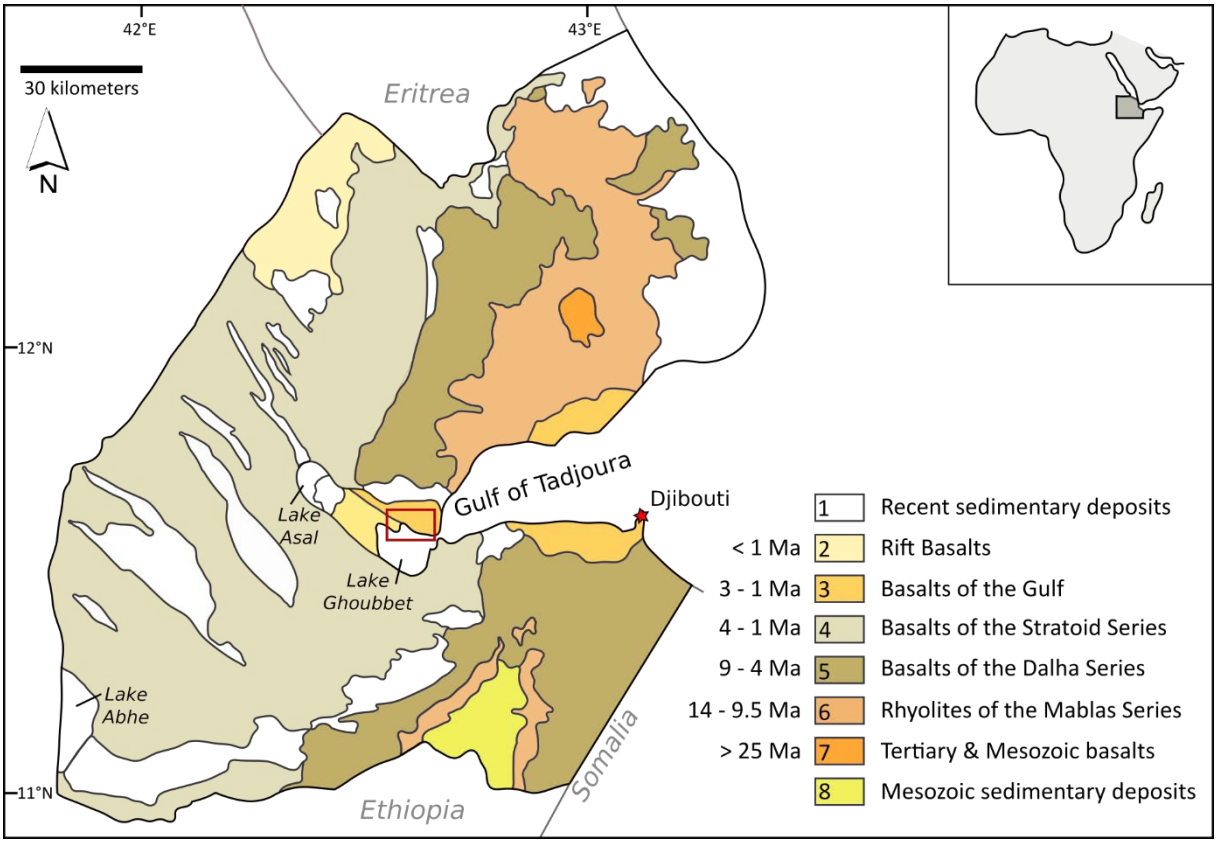

Figure 4.3: Simplified geological map of the Republic of Djibouti (modified after Vellutini 1990). The red rectangle shows the location of the study area North Ghoubbet.

4.2 Geology in North Ghoubbet

The study area North Ghoubbet is located north of Lake Ghoubbet (Figure 4.3). It is bordered by the Asal-Rift in the southwest and the Gulf of Tadjoura in the east. The North Ghoubbet area consists of two main rock groups from the geological units described above. The Basalts of the Gulf occur in the northeastern part and the Rift Basalts of the Asal Rift occur in a small part in the southwest (Figure 4.3, red rectangle).

Tectonic Structures in North Ghoubbet

The young rift basalts that cover the study area are largely dissected by faults of different directions, contributing to high permeability for hydrothermal fluids. As the working area is located in the Triple Junction, the tectonic activity is high resulting from active rift opening. Characteristics of the faults like sharp morphology suggest recent activity, and deformation records of several studies show the ongoing activity of many faults in the study area (Corti et al. 2015, Doubre et al. 2007, Doubre & Peltzer 2007).

The NW-SE trending Asal-Ghoubbet rift system borders the study area to the southwest. The rift system is linked to the also NW-SE trending Manda-Inakir rift further in the north by the N(NW)-S(SE) oriented Makarassou Fault Zone, acting as the transfer zone between the two

rift systems (Le Gall et al. 2011, Polun et al. 2018, Vellutini 1990). Figure 4.4a shows the location of the two rift systems and the Makarassou Fault Zone as their connection. This strike-slip fault zone is dominated by N-S oriented strike-slip faults intersecting with NW-SE striking fractures with directions varying from 150°-180° and steep dips of 70° to 80° towards the east (Le Gall et al. 2011, Manighetti et al. 2001, Vellutini 1990).

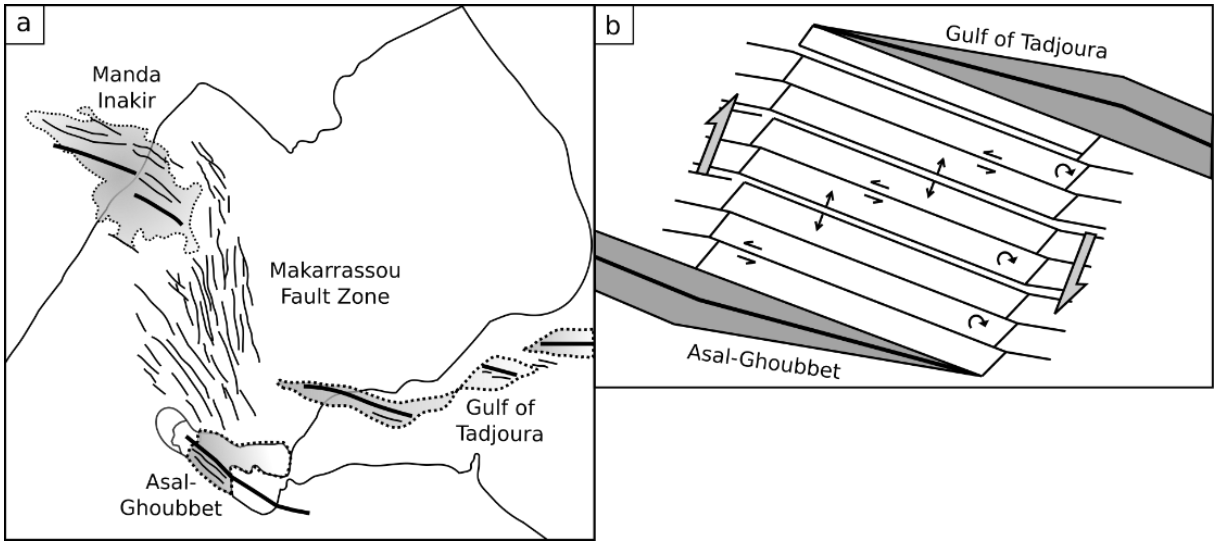

Figure 4.4: (a) Location of the Manda Inakir Rift, the Asal-Ghoubbet Rift and the Makarassou Fault Zone that connects the two rift systems as well as the Gulf of Tadjoura (modified after Vellutini 1990). (b) Bookshelf faulting in the overlapping zones of two rift systems, applied to the study area (after Manighetti et al. 2001, Tapponnier et al. 1990).

A paleomagnetic study by Manighetti et al. (2001) shows that block rotation takes place in the Asal-Ghoubbet area, resulting from the overlapping of different rift systems, as it is the case of the overlapping Asal-Ghoubbet Rift and the Gulf of Tadjoura (Manighetti et al. 2001, Tapponnier et al. 1990). Rotation is accommodated by a bookshelf faulting mechanism, where slipping occurs along a number of parallel faults. In this study area, the NW-SE oriented faults of the main direction represent the parallel faults that accommodate clockwise rotation by sinistral shear along the single structures. This mechanism is shown in Figure 4.4b.

Tectonic structures of a wider area around North Ghoubbet are already analysed by Manighetti et al. (2001) based on SPOT satellite imagery. The result of this study is shown in Figure 4.5 and defines NW-SE (310°-330°) trending structures as the major fault direction and NNW-SSE (330°-350°) structures as a secondary fault direction.

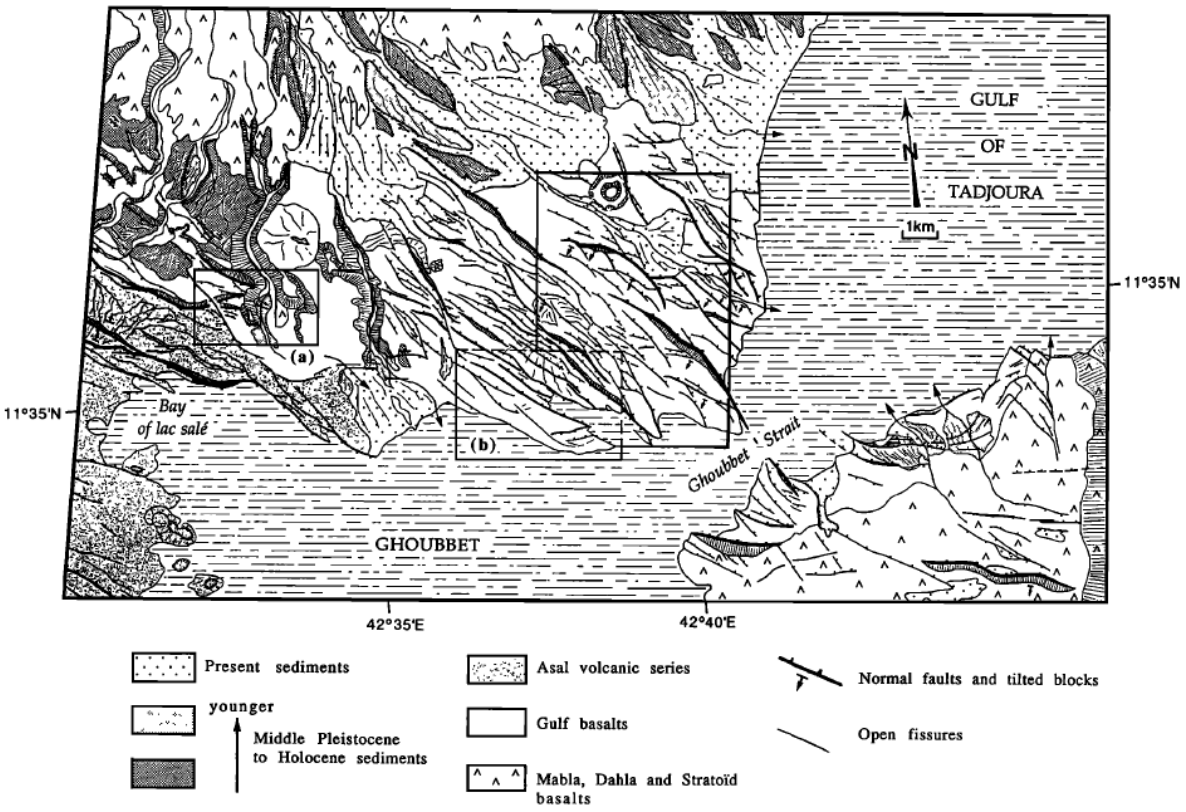

Figure 4.5: Geological and tectonic map of the larger North Ghoubbet area based on SPOT imagery, analyses conducted by Manighetti et al. 2001.

5 Lineament Analysis

5.1 Remote Sensing Data

The following data are used for further analysis and lineament vectorization in ArcGIS (Version 10.3.1).

1. Enhanced and geocoded satellite image:
    - Sentinel 2A (MSI) acquired October 23, 2019; 20 m ground resolution. The Sentinel-2 band characteristics are shown in Figure 5.1.

Band number	Central wavelength (nm)	Bandwidth (nm)	Spatial resolution (m)
1	443	20	60
2	490	65	10
3	560	35	10
4	665	30	10
5	705	15	20
6	740	15	20
7	783	20	20
8	842	115	10
8b	865	20	20
9	945	20	60
10	1380	30	60
11	1610	90	20
12	2190	180	20

Figure 5.1: Band characteristics of Sentinel-2 (ESA 2012).

2. Digital elevation model (DEM) from the Shuttle Radar Topography Mission (SRTM), 30 m resolution
3. Sentinel-1 amplitude imagery
4. Information from overview-field work (February 2020):
    - Shape and visibility of lineaments,
    - Additional geological and tectonic information,
    - Field photos,
    - Waypoints (WP): GPS measurements of findings.

For all data, the spatial reference system UTM 38 N, WGS 84 was used. Image enhancement and shaded relief generation was conducted with the Software ENVI 5.5.

The following thematic layers have been created and are attached to this report:

- Shaded relief maps
- Enhanced Sentinel-2A multispectral image
- Sentinel 1 amplitude imagery
- Waypoints with corresponding data tables concerning information from fieldwork

- Lineaments, major
- Lineaments, minor
- Study area

A QGIS project containing these layers is attached to this report.

5.2 Lineaments

The lineament analysis was conducted based on SRTM digital elevation data, Sentinel-2 multispectral images and Sentinel-1 amplitude imagery. Amplitude images are very useful in structural studies, as radar sensors, which penetrate the ground in cm-scale, acquire this information. Therefore, they may reveal information that is not visible on multispectral imagery or DEMs. The result of the lineament mapping is shown in Figure 5.2 and the corresponding rose diagram for all mapped lineaments is shown in Figure 5.3.

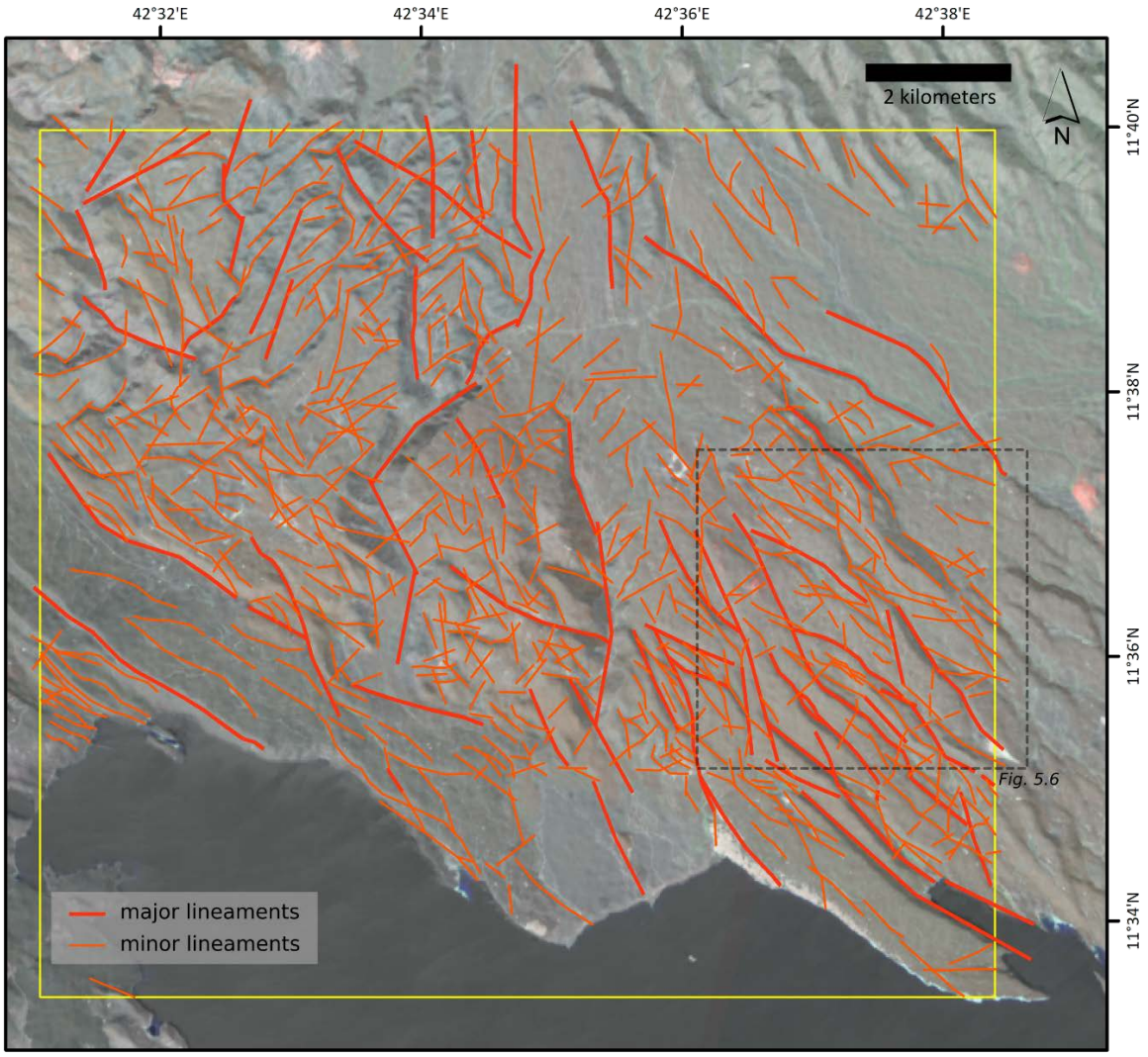

Figure 5.2: Lineaments (red) in the study area (yellow). Sentinel-2 scene (band combination 12-8a-5) transparent on the shaded relief model in the background (Contains modified Copernicus Sentinel data 2019). The grey rectangle shows the location of Figure 5.6.

The rose diagrams in the following figures are generated by using the *QGIS Line Direction Histogram Plugin* in QGIS Version 3.6.3. They show the distribution of structures in intervals of 15°. The number of lineaments occurring in each of these intervals determines the length of the single bins without weighting the lineament length. Additionally, the direction mean is calculated and represented by a red colored bin in the diagrams. The calculation of this direction mean only takes into account the number of lineaments in the single intervals and not

their length. The strength of the direction mean accords to the intensity of the red color. Thus, in rose diagrams where the primary direction is very dominant and only a few lineaments occur in other directions, the direction mean is very distinct and appears in an intense red color, while in rose diagrams where lineaments spread in several directions, the direction mean is less well pronounced with a weak coloring.

In summary, 1630 lineaments are mapped (Figure 5.3a). The longest lineament accounts for 2158 meters without changing direction. The major direction is NW-SE (300°). The adjacent directions, especially further towards the north (315°) are well pronounced as well. A secondary direction of NE-SW (45°) oriented lineaments represents conjugated structures. The mean direction value, represented by the red colored bin in the rose diagram, corresponds to the main direction NW-SE, showing a slight tendency towards the north.

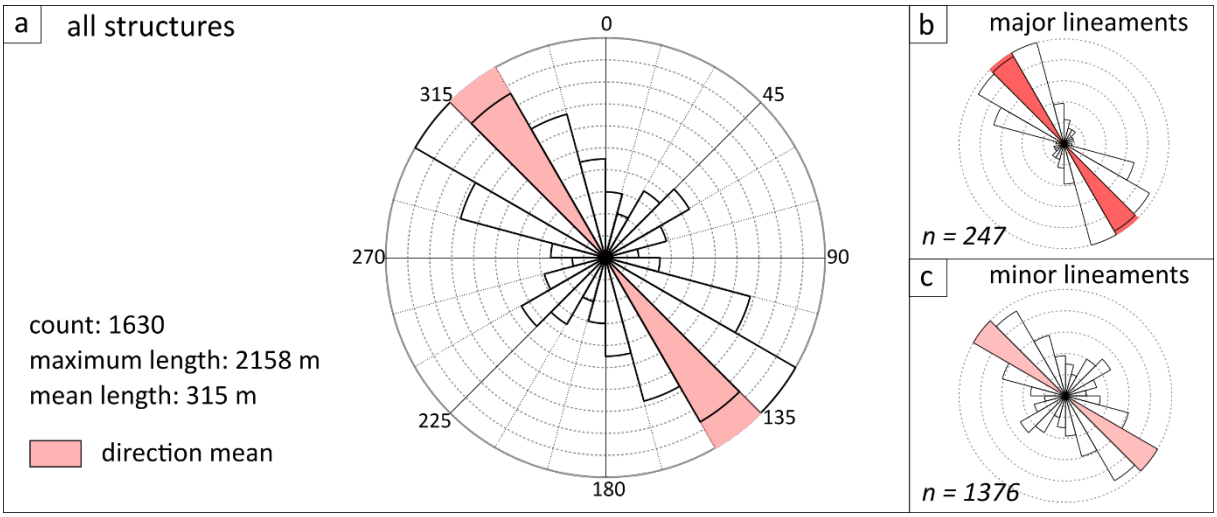

Figure 5.3: (a) Rose diagram of all structures in the study area with the main direction 300° NW-SE. A secondary direction with 45° NE-SW is recognizable, although not as well pronounced as the primary direction. The direction mean is indicated by the red-colored bin. (b) Rose diagram of major lineaments almost only showing NW-SE oriented structures. (c) Rose diagram of minor lineaments including both the primary NW-SE and secondary NE-SW direction.

The lineaments are categorized as major and minor structures. Major structures are lineaments that are continuous over several hundreds of meters up to 2 kilometers and that significantly control the geomorphology of this area. This is determined by using a slope map generated from the DEM as shown in Figure 5.4.

The separate rose diagrams for major and minor lineaments are similar, showing a primary NW-SE orientation (Figure 5.3b & c); although the major structures also contain a considerable amount of NNW-SSE oriented lineaments. The secondary NE-SW direction is almost merely represented in the rose diagram of minor lineaments.

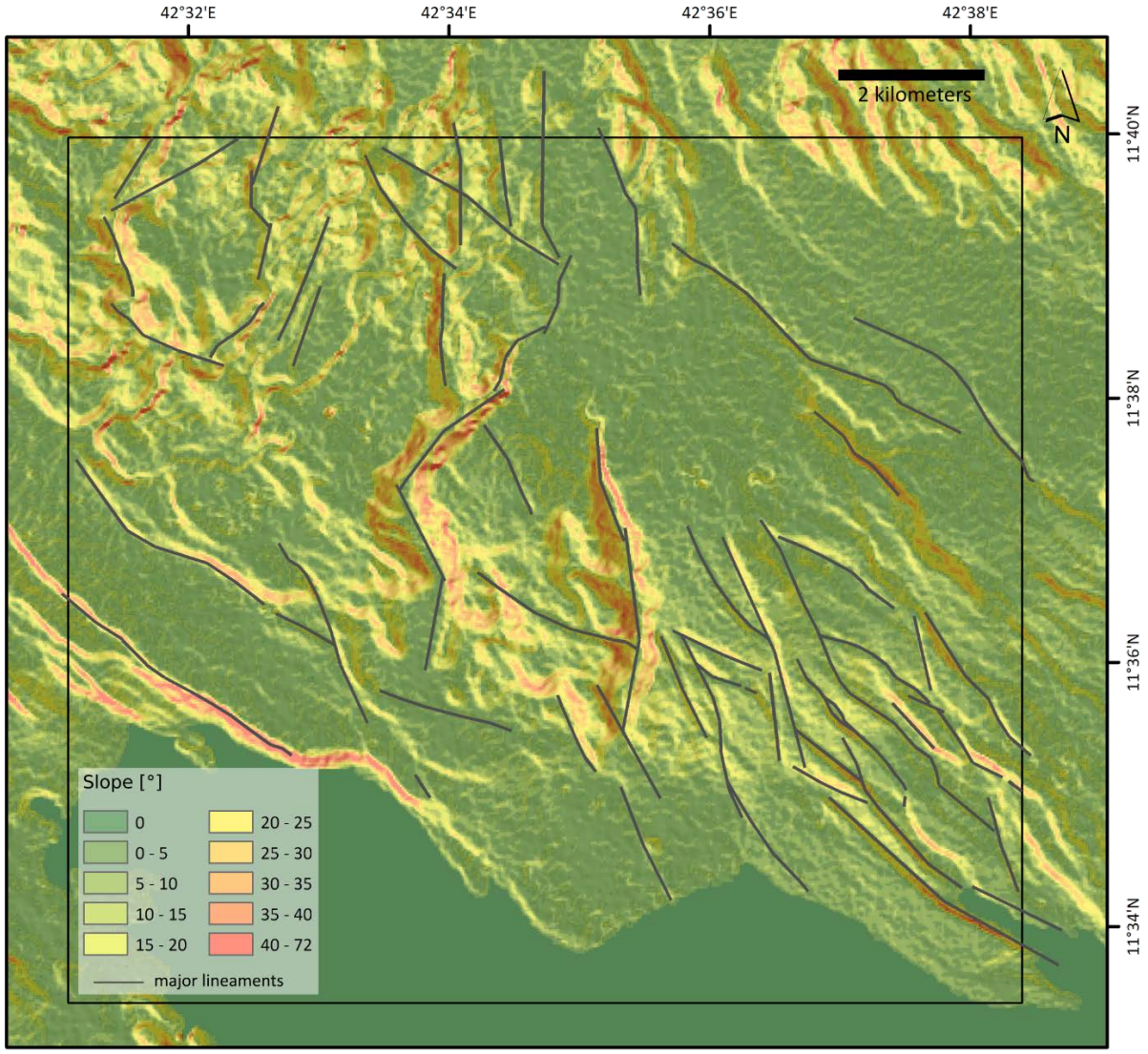

Figure 5.4: Slope map (generated from the DEM) that is used for the determination of major and minor lineaments.

As described in Chapter 4, different tectonic systems influence the orientations of structures in the study area. A development of lineament directions slightly is observable on the lineament map in Figure 5.2. To evaluate if there is a notable development in lineament orientations, e.g. from north to south or east to west, the study area is separated into nine single tiles as shown in Figure 5.5. The number of tiles or, respectively, their size is chosen based on the length of major lineaments, as they represent the major structural control of the area. Figure 5.5 includes rose diagrams, the number of lineaments as well as the number of lineament intersections per tile. The concentration of lineaments and lineament intersections in specific areas are a useful indicator for enhanced permeability.

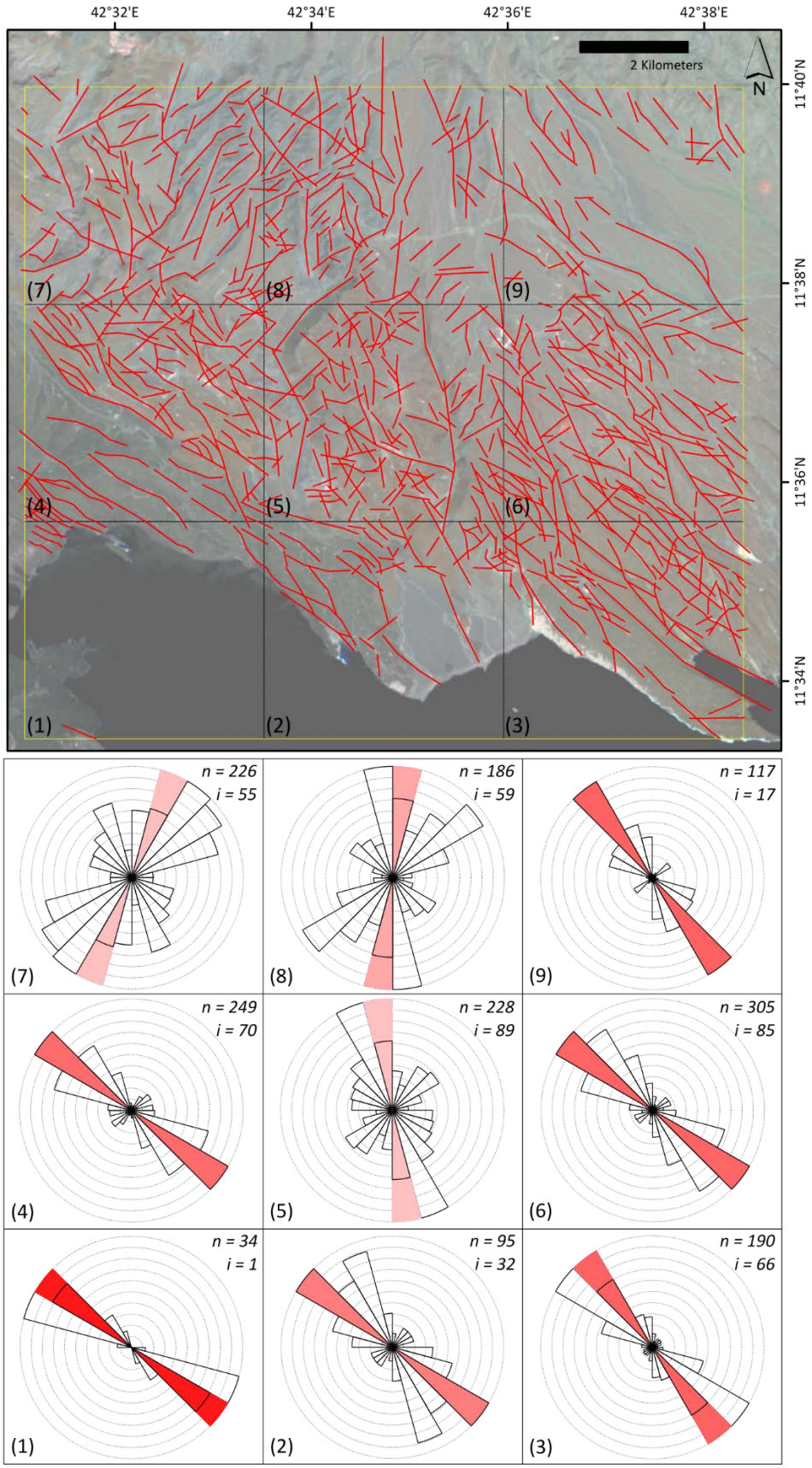

Figure 5.5: Study area divided into nine tiles with the corresponding rose diagrams for each tile. The red bins represent the mean direction values while the intensity of the color shows the strength of the mean values. The mean direction is less pronounced in rose diagrams with many different directions. n is the number of lineaments per tile, i the lineament intersection per tile. (Contains modified Copernicus Sentinel data 2019).

The rose diagrams show clear variations, although the major direction of NW-SE (300°) structures is visible in each single diagram (Figure 5.5). In the southernmost diagrams (1), (2), and (3), the major NW-SE (300°) direction is well pronounced and the direction mean (red bin) is very distinct due to small numbers of lineaments in other directions. Rose diagram (2) shows a secondary direction of NNW-SSE (330°). Rose diagrams (4), (5) and (6) show similar characteristics. While the eastern and western diagrams (4) and (6) mainly show the NW-SE (300°) direction, the central rose diagram (5) clearly shows a tendency towards more northerly oriented structures. Additionally, the other directions are present as well, leading to a less significantly pronounced direction mean (lighter red color). Diagrams (7) and (8) differ from the other diagrams in their major direction. Diagram (7) shows a well pronounced NE-SW (30°) direction and NW-SE (330°) as a secondary direction. The major direction in diagram (8) is NNW-SSE (345°), while the secondary direction NE-SW (30°) is also well pronounced. Diagram (9) corner shows a distinct NW-SE (315°) major direction.

In conclusion, there are several characteristics observable revealing different tectonic influences. Lineaments are mainly oriented NW-SE (300°), while conjugated structures appear approximately 100° shifted in a NE-SW (45°) oriented direction. This shows that the study area is mainly influenced by the active NW-SE trending Asal-Ghoubbet Rift system that borders the study area to the southwest. In some rose diagrams, the NE-SW (45°) direction is appearing remarkably well pronounced**.**

The major NW-SE direction develops from 300° in the southern part of the area towards a more northerly trend of 315° in the northern part of the study area, indicating that the influence of the N(NW)-trending Makarassou fault zone increases towards the north(west). From south to north, the dominance of the major NW-direction decreases. Towards the north, a higher number of structures appears in other directions. This is especially observable towards the northwest, as diagrams (7) and (8) show the least distinctive direction means (lightest red). In addition, diagram (5) includes structures of many different directions as well. It can be deduced that with increasing distance from the Asal-Ghoubbet rift, the influence of other tectonic systems, especially the Makarassou Fault Zone, increases as well.

5.3 Indicators for the Direction of Shear

There are different features that can be observed in the mapped lineaments giving information about the direction of shear. The structures occurring in North Ghoubbet indicate a sinistral sense of shear. Features indicating this sinistral shear are sketched on Figure 5.6a. There are three different types of indicators: right stepping segmentation, pull-apart structures and horsetail structures. To demonstrate the appearance of these indicators, they are illustrated for a small extent in the eastern part of the study area (Figure 5.6b & c). The right stepping segmentation of faults often appears in combination with pull-apart structures that are developed to different degrees.

Horsetail structures are characterized by the bending of faults (Figure 5.6), which is a very distinctive and prevalent phenomenon in the whole study area. Similar structures where described by Manighetti et al. 2001. The sinistral shear results from the process of bookshelf faulting that was described earlier.

Indicators for sinistral shear

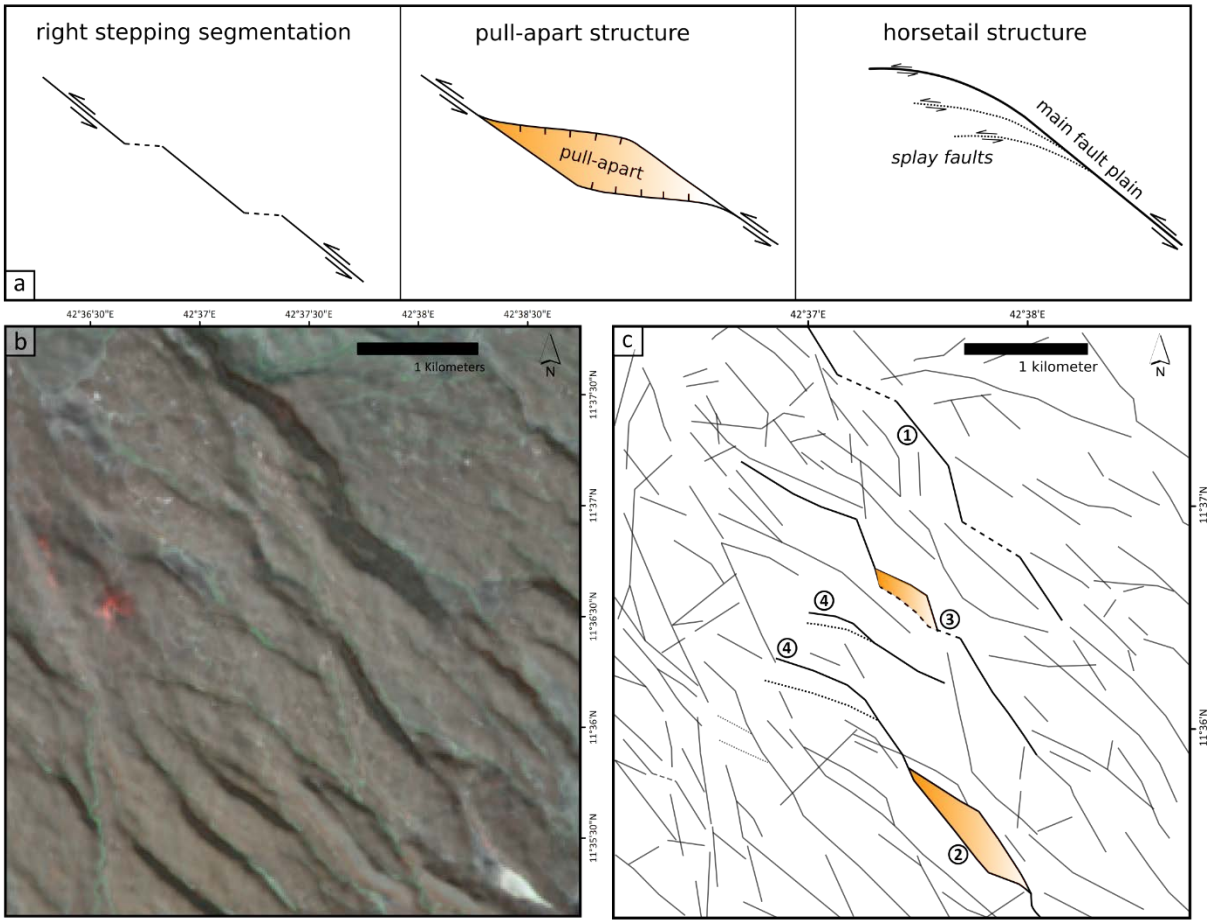

Figure 5.6: Indicators for sinistral shear. (a) Schematic sketches of the indicators of right stepping segmentation of faults, pull-apart structures and horsetail structures. (b) Small extent in the eastern part of the study area. The location of this extent is shown in Figure 5.2. Sentinel-2 band combination 12-8a-5 transparent on a shaded relief model (225° illumination direction) (Contains modified Copernicus Sentinel data 2019). (c) Lineaments of the extent shown in (b) with movement indicators of right-stepping faults (1), pull-apart structures (2), a combination of both (3) and horsetail structures (4).

6 Field Evidence

The study area was surveyed in February 2020 (10. - 12.02.2020), with focus on the central part of the area. Numerous geothermal manifestations are discovered, especially in the area located between Wadi Afay and Wadi Analé. This area is mainly represented by the defined sub-area 5, where lineaments occur in several directions (Figure 5.2, Figure 5.5).

In most cases, the manifestations are fumaroles occurring in alteration zones with several meters length and width, characterized by intense alteration of the basaltic bedrock (Figure 6.1). The altered materials exist of iron-rich clay minerals, giving the fumarolic outcrops a spectacular red color. Sulphurous as well as calcitic crystallizations occur in very small amounts and as small-area incrustations in the surroundings of fumarolic sites.

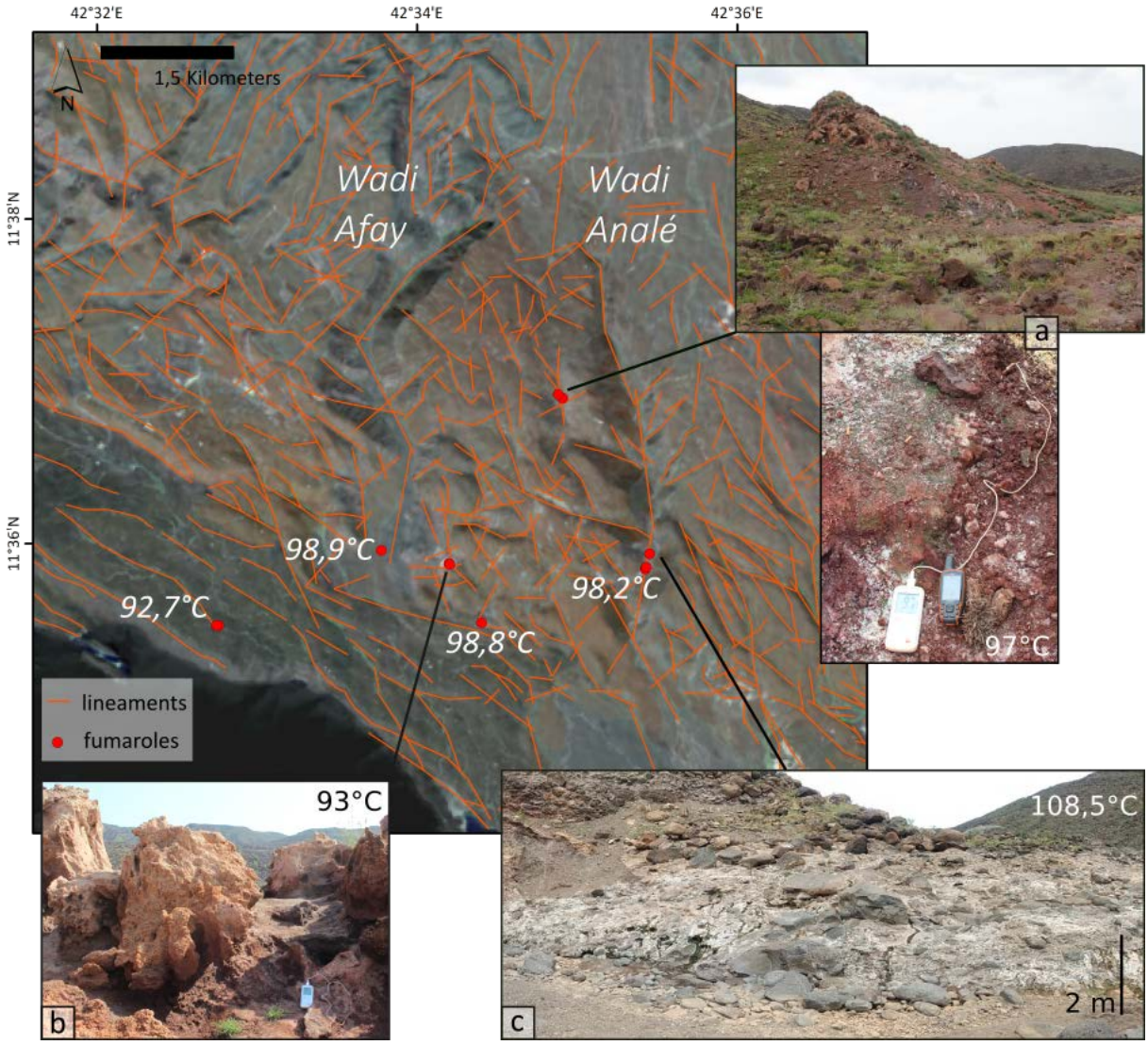

Figure 6.1: Map of the central part of the study area with lineaments in orange and the location of fumaroles as red points with the measured temperatures. Background: Sentinel-2A image transparent on a shaded relief model (Contains modified Copernicus Sentinel data 2019). Fumaroles (a) and (b) show the most common appearance of fumaroles with the surrounding red-colored iron rich alteration. (c) Most extensive manifestation with the highest temperature of 108,5°C.

The fumarolic activity appears without any steam, vapor or water (Figure 6.1). At one location in the eastern part of the study area in Wadi Analé**,** hot water reaches the surface. This hot spring location exhibits the highest measured temperature of 108.5°C (Figure 6.1c), while temperatures at other locations range between 90°C and 100°C (Figure 6.1).

The discovered fumaroles occur along intersections of NW-SE striking lineaments of the major direction with NNW-SSE striking lineaments of the secondary direction, as for example fumaroles (a) and (b) in Figure 6.1. Other fumaroles are located along the traces of NW-SE and N-S oriented structures. Large structures control the orientation of the extensive wadi systems Wadi Afay and Wadi Analé in the central part of the study area. Surface manifestations are located along their walls, indicating that the structures controlling the wadi systems play a significant role in the transport of hydrothermal fluids. These structures probably extend to high depth and act as major pathways in this system.

The location of the most extensive geothermal hot spring manifestation with temperatures up to 108.5°C right in the center of Wadi Analé extending over several tens of meters in length along the wadi channel supports this assumption.

A table with the coordinates and temperature measurements of the geothermal manifestations and a corresponding map with their locations are attached in the appendix.

7 Conclusion and Recommendation

The tectonic framework of the investigated area is influenced by large systems of the active rifts Asal-Ghoubbet and Manda Inakir with the Makarassou Fault Zone acting as a transfer zone between them. These huge regional systems slightly differ in their orientations, leading to the development of faults in the directions NW-SE and N(NW)-S(SE). They also favor the continuation of faults in high depths, resulting in good conditions for the development of a system permitting significant fluid circulation. Most lineaments follow these two directions, and fumaroles mostly occur at intersections of lineaments with these directions. For locating hydrothermal activity, it is recommendable to focus on locations where the NW-SE and N-S structures intersect.

Figure 7.1 shows the areas suitable for additional investigations, these areas are described in the following. They are defined based on lineament density, lineament directions and the occurrence of lineament intersections.

As already described in Chapter 5.2 *Lineaments*, especially the central and eastern parts of the study area are characterized by a dense lineament network with a high variety of tectonic directions and consequently a large amount of lineament intersections. Referring to Figure 5.5, sub-area 5 and sub-area 6 cover these parts. In the central part of the working area, represented by sub-area 5 in Figure 5.5, geothermal manifestations prove evidence for the circulation of geothermal fluids, being favored by the deeply incising fault controlled wadi systems Wadi Afay and Wadi Analé.

A small area west of Wadi Afay is depicted as *Recommended Area A* in Figure 7.1, as is of interest due to several intersections along two N(NW)-S(SE) striking structures and the vicinity to the above mentioned wadi system and to one of the observed fumaroles.

A major NW-SE striking lineament, marked as lineament ε in Figure 7.1b, can be traced from the central part of the study area towards the in the southeast crossing Wadi Analé. The occurrence of geothermal manifestations along Wadi Analé is already proven, therefore the area marked as *Recommended Area B* in Figure 7.1 that surrounds lineament ε is found to be interesting for locating further manifestations, as this major lineament possibly plays a significant role for fluid circulations as well.

East of Wadi Analé, in an area that is mostly covered by sub-area 6 in Figure 5.5, major lineaments occur in high density and with a large number of intersections. This area is recommended for further analysis, as geothermal manifestations might occur with high probability along the NW-SE striking structures. *Recommended Area C* in Figure 7.1 marks the area where major lineaments lie closely together and that is therefore well-suited for further analysis and for locating further geothermal activity.

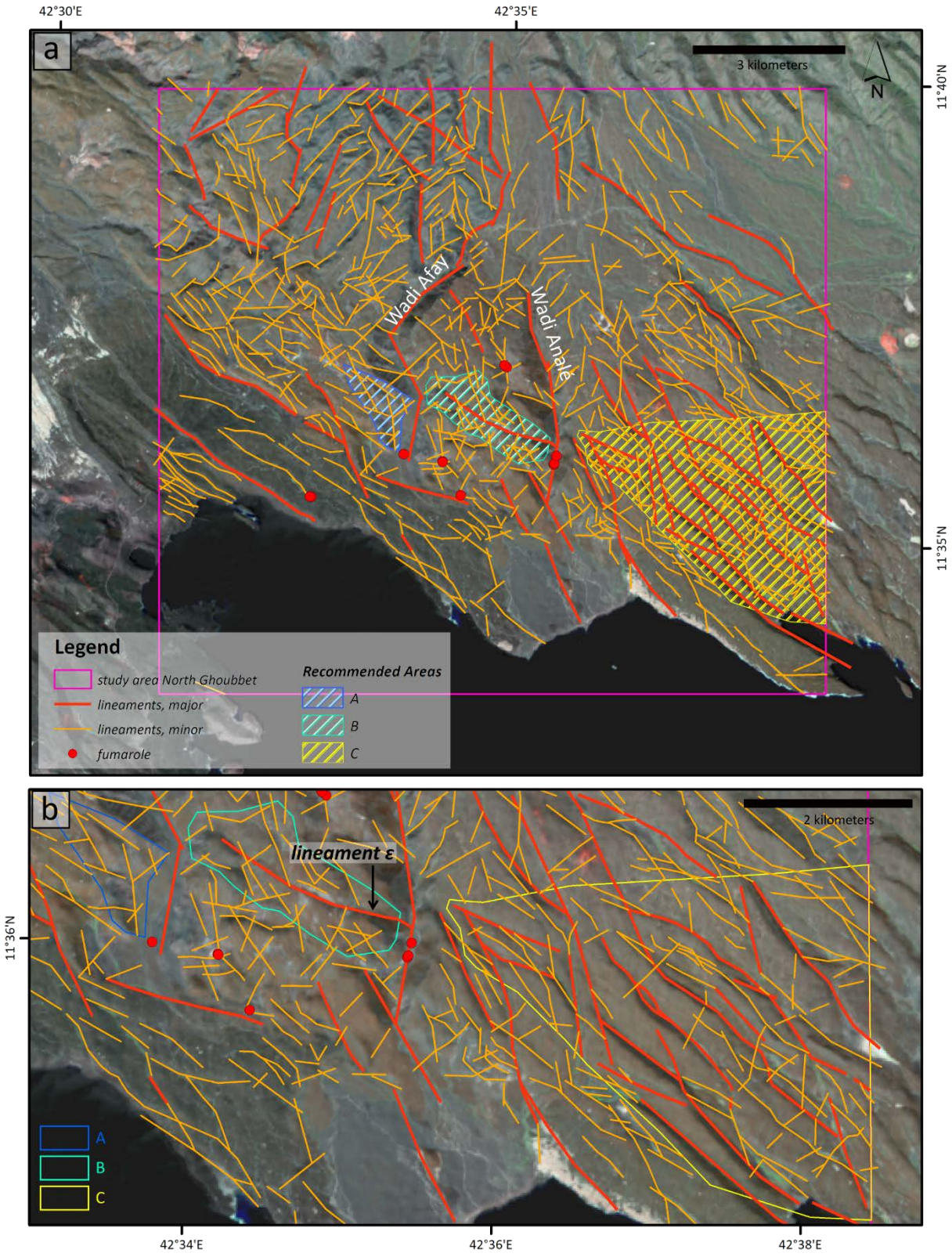

Figure 7.1: Recommended areas for further investigations in the whole study area (a) and zoomed in (b). Contains modified Copernicus Sentinel data 2019.

8 Outlook

Results of the lineament analysis lead to the identification of prospective areas. Additional studies like InSAR analysis, drone surveys and the integration of high-resolution satellite imagery should be used for a further limitation of the areas.

The location and accumulation of geothermal manifestations gives insight into the activity of specific tectonic structures. To expand the knowledge about structures facilitating fluid circulation, an InSAR analysis is performed based on Sentinel-1 data. This method enables the detection of ground motions in a millimeter-scale that, beside of tectonic activity, may indicate magmatic activity or fluid circulation in near-surface zones.

The field work shows that geothermal manifestations are widely associated with the occurrence of alteration zones. Detailed mapping of these altered zones helps locating additional manifestations and in turn defining areas of high geothermal activity even more precisely than it could be defined only by lineament analysis based on Sentinel-2 and SRTM data. As the alteration zones are mainly just a few meters in extension, this mapping cannot be applied on freely available remote sensing data (e.g. Sentinel-2) due to their coarse resolution. For this investigation, high-resolution satellite imagery with suitable spatial and spectral resolution is acquired.

For the interpretation and rating of the geothermal potential, a detailed mapping of thermal anomalies, either by satellite imagery or by including drone surveys in further exploration studies, would support the lineament analysis and the subsequent alteration mapping very well.

9 References

Aden, M., Koichiro, W., Thomas, T. (2018). Sub-surface geology of hydrothermal alteration and 3D geological model of the wells GLC-1, ASAL 3, 4, and 5 in Asal-Rift geothermal field, Djibouti. Proceedings of 7th African Rift geothermal Conference.

Beyene, A., & Abdelsalam, M. G. (2005). Tectonics of the Afar Depression: A review and synthesis. *Journal of African Earth Sciences*, *41*(1-2), 41-59.

Chorowicz, J. (2005). The east African rift system. *Journal of African Earth Sciences*, *43*(1-3), 379-410.

Collet, B., Taud, H., Parrot, J. F., Bonavia, F., & Chorowicz, J. (2000). A new kinematic approach for the Danakil block using a Digital Elevation Model representation. *Tectonophysics*, *316*(3-4), 343-357.

Corti, G., Bastow, I. D., Keir, D., Pagli, C., & Baker, E. (2015). Rift-related morphology of the Afar Depression. In *Landscapes and Landforms of Ethiopia* (pp. 251-274). Springer, Dordrecht.

De Chabalier, J. B., & Avouac, J. P. (1994). Kinematics of the Asal Rift (Djibouti) determined from the deformation of Fieale Volcano. *Science*, *265*(5179), 1677-1681.

Doubre, C., Manighetti, I., Dorbath, L., Dorbath, C., Bertil, D., & Delmond, J. C. (2007). Crustal structure and magmato-tectonic processes in an active rift (Asal-Ghoubbet, Afar, East Africa): 2. Insights from the 23-year recording of seismicity since the last rifting event. *Journal of Geophysical Research: Solid Earth*, *112*(B5).

Doubre, C., & Peltzer, G. (2007). Fluid-controlled faulting process in the Asal Rift, Djibouti, from 8 yr of radar interferometry observations. *Geology*, *35*(1), 69-72.

Eagles, G., Gloaguen, R., & Ebinger, C. (2002). Kinematics of the Danakil microplate. *Earth and Planetary Science Letters*, *203*(2), 607-620.

ESA. 2012. Sentinel-2: ESA's Optical High-Resolution Mission for GMES Operational Services (ESA SP-1322/2 March 2012). ESA Communications, Noordwijk.

Houssein, D. E., & Axelsson, G. (2010). Geothermal resources in the Asal Region, Republic of Djibouti: An update with emphasis on reservoir engineering studies. *Geothermics*, *39*(3), 220-227.

Le Gall, B., Daoud, M. A., Rolet, J., & Egueh, N. M. (2011). Large-scale flexuring and antithetic extensional faulting along a nascent plate boundary in the SE Afar rift. *Terra Nova*, *23*(6), 416-420.

Manighetti, I., Tapponnier, P., Courtillot, V., Gallet, Y., Jacques, E., & Gillot, P. Y. (2001). Strain transfer between disconnected, propagating rifts in Afar. *Journal of Geophysical Research: Solid Earth*, *106*(B7), 13613-13665.

McClusky, S., Reilinger, R., Ogubazghi, G., Amleson, A., Healeb, B., Vernant, P., Sholan, J., Fisseha, S., Asfaw, L., Bendick, R., & Kogan, L. (2010). Kinematics of the southern Red Sea–Afar Triple Junction and implications for plate dynamics. *Geophysical Research Letters*, *37*(5).

Pinzuti, P., Mignan, A., & King, G. C. (2010). Surface morphology of active normal faults in hard rock: Implications for the mechanics of the Asal Rift, Djibouti. *Earth and Planetary Science Letters*, *299*(1-2), 169-179.

Polun, S. G., Gomez, F., & Tesfaye, S. (2018). Scaling properties of normal faults in the central Afar, Ethiopia and Djibouti: Implications for strain partitioning during the final stages of continental breakup. *Journal of Structural Geology*, *115*, 178-189.

Sani, F., Ghinassi, M., Papini, M., Oms, O., & Finotello, A. (2017). Evolution of the northern tip of Afar triangle: Inferences from the Quaternary succession of the Dandiero—Massawa area (Eritrea). *Tectonophysics*, *717*, 339-357.

Schlüter, T. (2008). *Geological atlas of Africa* (p. 307). Springer-Verlag, Berlin.

Tapponnier, P., Armijo, R., Manighetti, I., & Courtillot, V. (1990). Bookshelf faulting and horizontal block rotations between overlapping rifts in southern Afar. *Geophysical Research Letters*, *17*(1), 1-4.

Tarikhi, P. (2012). InSAR of aquatic bodies. International Archives of the Photogrammetry, Remote Sensing and Spatial Information Sciences; ISPRS Congress, 25 August –01 September, Melbourne, Australia.

Vellutini, P. (1990). The Manda—Inakir rift, republic of Djibouti: A comparison with the Asal rift and its geodynamic interpretation. *Tectonophysics*, *172*(1-2), 141-153.

Vigny, C., de Chabalier, J. B., Ruegg, J. C., Huchon, P., Feigl, K. L., Cattin, R., Asfaw, L., & Kanbari, K. (2007). Twenty-five years of geodetic measurements along the Tadjoura-Asal rift system, Djibouti, East Africa. *Journal of Geophysical Research: Solid Earth*, *112*(B6).

Zan, L., Gianelli, G., Passerini, P., Troisi, C., & Haga, A. O. (1990). Geothermal exploration in the Republic of Djibouti: thermal and geological data of the Hanlé and Asal areas. *Geothermics*, *19*(6), 561-582.

10 Appendix

10.1 Field work - Waypoints and Map

Waypoints of measurements and field photos as mentioned in figures. The datum of the coordinates (Decimal degrees and UTM zone 16N) is WGS84.

WP	Latitude	Longitude	Type	Temperature [°C]	Date
01	42.573977	11.592250	fumarole	98.9	10.02.2020
02	42.570544	11.598300	fumarole	98	10.02.2020
03	42.570615	11.598229	fumarole	93	10.02.2020
04	42.563473	11.599594	fumarole	98.9	10.02.2020
05	42.546846	11.591433	alteration		10.02.2020
06	42.546636	11.591756	fumarole	82.2	10.02.2020
07	42.546386	11.591766	fumarole	92.7	10.02.2020
08	42.546288	11.591968	alteration		10.02.2020
09	42.582217	11.615384	fumarole	97	11.02.2020
10	42.581754	11.615767	fumarole	94.8	11.02.2020
11	42.582421	11.613914	alteration		11.02.2020
12	42.586852	11.610445	alteration		11.02.2020
13	42.589720	11.613063	alteration		12.02.2020
14	42.589268	11.590554	alteration		12.02.2020
15	42.590250	11.592366	fault		12.02.2020
16	42.590094	11.596734	alteration		12.02.2020
17	42.590965	11.597921	fumarole	98.2	12.02.2020
18	42.591071	11.598126	fumarole	98.7	12.02.2020
19	42.591425	11.599485	fumarole	108.5	12.02.2020

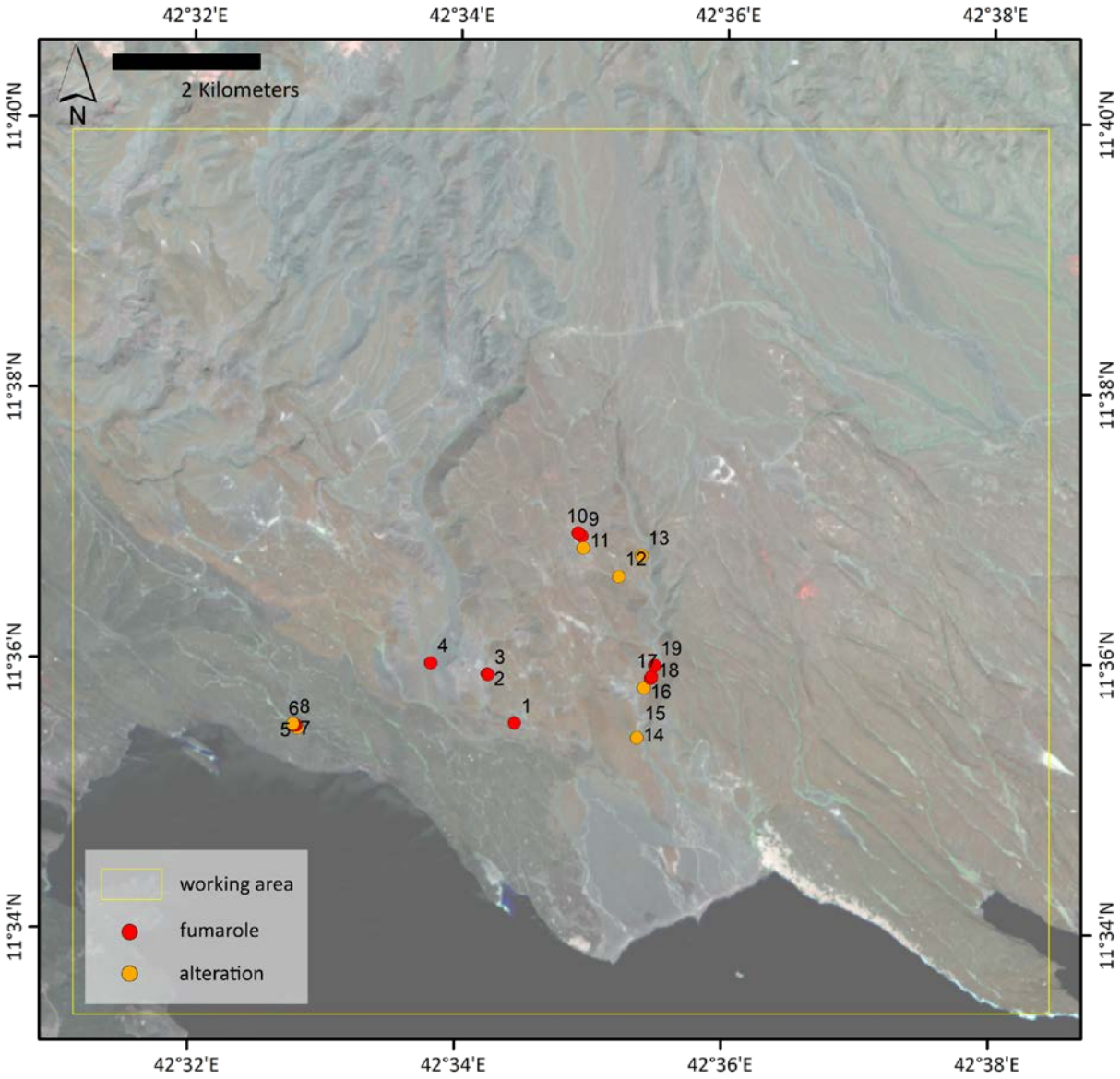
42°32'E
42°34'E
42°36'E
42°38'E
11°40'N
11°38'N
11°36'N
11°34'N
2 Kilometers
N
10
9
11
13
12
4
3
2
1
19
17
18
16
15
14
6
8
5
7
working area
fumarole
alteration